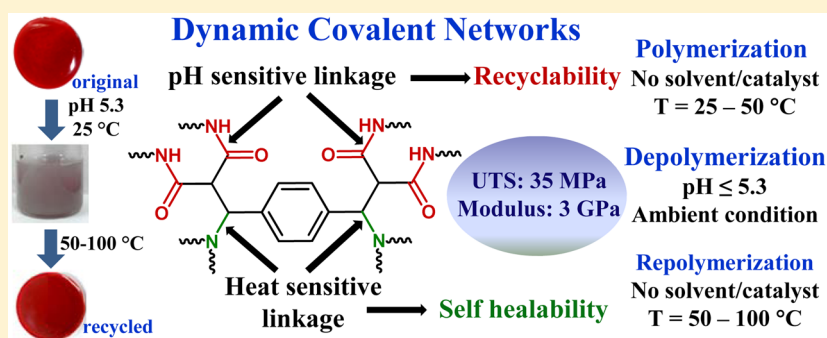


Recyclable Thermosets Based on Dynamic Amidation and Aza-Michael Addition Chemistry

Ranjana Baruah,[†] Anuj Kumar,[†] Rewati Raman Ujjwal,[†] Soumya Kedia,[‡] Amit Ranjan,[‡] and Umapasana Ojha^{*†}

[†]Department of Chemistry and [‡]Department of Chemical Engineering, Rajiv Gandhi Institute of Petroleum Technology, Rae Bareilly, UP 229316, India

S Supporting Information



ABSTRACT: Utilizing the dynamic amidation and aza-Michael addition chemistry, a set of high strength, recyclable, and self-healable covalent adaptable networks (CANs) are synthesized by reacting the precursor and commercial oligoamine cross-linkers under mild temperature (25–50 °C) and solvent-free conditions. The amide linkages present in these CANs are readily hydrolyzable under mild acidic (pH = 5.3) conditions, whereas the aza-Michael adducts with secondary amines are thermally reversible. Utilizing the above, these CANs are depolymerized under ambient conditions in mild acidic solution and recycled with retention of original mechanical properties. The crack on the material surface is self-healed at 50 °C. The precursor, a Knoevenagel condensation product of terephthalaldehyde and diethyl malonate, is easily synthesized in a large scale. Suitable model compounds are synthesized and studied to further understand the transformations involved in the polymerization–depolymerization of these networks. These networks exhibit adequate tensile properties (ultimate tensile strength ≤35 MPa and Young’s modulus ≤3 GPa), and the properties can be tuned further by suitably changing the oligoamine cross-linker. The simplicity of synthesis, cost effectiveness, adequate mechanical property, stability in aqueous and organic media, and recyclability along with self-healability render these CANs suitable for a range of applications.

INTRODUCTION

The growing concern over global accumulation of plastic debris has motivated the development of recyclable and degradable plastics possessing dynamic or labile linkages.^{1,2} Macromolecules based on dynamic covalent linkages exhibit remarkable material properties such as stimuli responsiveness,^{3,4} adaptiveness,^{5,6} shape memory characteristic,⁷ self-healability,^{8,9} and reinforcement in mechanical properties.^{10,11,12} Fascinating examples of dynamic covalent chemistries based on the imine,^{13,14} hemiaminal,^{15,16} acyl hydrazones,^{17,18} oxime,^{19,20} hemiacetals,²¹ quaternary ammonium salt,²² boronic ester,²³ and trans-esterification²⁴ linkages are available in current literature.^{25,26} External stimuli such as temperature,^{27,28} pH,²⁹ light,^{30,31} and enzyme³² are generally utilized to control the dynamicity of these labile linkages. Though the vitrimer approach is particularly useful to induce dynamic character in networks by simply controlling the temperature,^{33,34} the temperature susceptibility of the cross-link acts as a deterrent toward use of these materials under variable temperature

conditions.^{35,36} Therefore, dynamic cross-links stable to various temperature conditions and susceptible to stimuli such as pH and chemicals could be advantageous for specific applications.³⁷ Moreover, the concept of using multiple types of dynamic linkages possessing responsiveness toward different stimuli in a covalent adaptable network (CAN) is advantageous to regulate the material properties.

Amide linkages are frequently incorporated in pharmaceuticals,³⁸ biologically active compounds, and polymers³⁹ and considered as one of the prevalent transformations in synthetic organic chemistry.^{40,41} These linkages are generally known to be stable to various temperature and pH conditions.⁴² Interestingly, the above linkage could be made readily degradable by suitably substituting the α carbon⁴³ or inducing steric strain at the “N” of the amide functionality.⁴⁴ The

Received: August 19, 2016

Revised: September 21, 2016

presence of an electron-withdrawing substituent at the α -carbon is known to promote the hydrolysis of amide functionality under mild acidic conditions through protonation of the amide "N" atom.^{45,46} Therefore, networks possessing activated amide linkages may be recycled using pH as the stimulus. Similarly, reversibility of Michael addition offers another possibility of being employed in the development of CANs. However, retro aza-Michael addition typically requires an additional reagent or catalyst and specific reaction conditions and therefore is not suitable for synthesis of CANs.⁴⁷ Recently, reversibility under noncatalytic and ambient conditions was introduced into thiol Michael addition by enhancing the electron deficiency of the double bond through conjugation with carboxylate and cyano functionality.^{48,49} A similar approach could also possibly be employed to induce thermal reversibility into the aza-Michael addition between amine functionality and activated double bond. Moreover, the cost-effectiveness of the precursor, suitability of the reaction condition, and kinetics of forward and reverse reaction is important for an effective design of a dynamic network.

Considering the above, a precursor capable of forming hydrolyzable amide linkage and reversible aza-Michael adduct is designed and synthesized. The precursor, a Knoevenagel condensation product of terephthalaldehyde and diethyl malonate (DEM) consisting of four carboxylate functionality and two highly activated double bonds, is cross-linked with a set of oligo-amines to synthesize the CANs. The depolymerization of the synthesized CANs is studied under mild acidic conditions, and their self-healability in the presence of thermal stimulus is explored. Suitable model compounds are synthesized and studied to understand the chemical transformations associated with the formation and degradation of these networks.

EXPERIMENTAL SECTION

Materials. Terephthalaldehyde (Across Organics, 98%), piperidine (Qualigens, 99.0%), acetic acid (s-d fine chem., 99.5%), DEM (s-d fine chem., 98%), *n*-butylamine (Fisher Scientific, >99.5%), diethylamine (Fisher Scientific, >99.5%), ethanol (Merck, 99.9%), dimethyl sulfoxide (DMSO, Merck, 99.5%), *N*-methylpyrrolidone (NMP, SRL Chem., 99.5%), tetrahydrofuran (THF, Rankem, 99.5%), sodium hydroxide (Qualigens, 98.0%), methanol (Qualigens, 99.0%), sodium bicarbonate (NaHCO₃, Merck, ≥99.0%), triethylenetetramine (TETA, Alfa Aesar, 60%), chloroform (CHCl₃, s-d fine chem., 99.5%), sodium sulfate (Na₂SO₄, Rankem, 99%), diethylenetriamine (DETA, s-d fine chem., 97%), pentaethylenhexamine (PEHA, Across Organics, 69.5%), and tetraethylenepentamine (TEPA, Across Organics) were used as received.

Characterization. ¹H and ¹³C NMR spectra were obtained on a Bruker AMX-500 spectrometer using CDCl₃ as a solvent and tetramethylsilane (TMS) as internal standard (δ H 0.00). The ¹H and ¹³C NMR spectra were recorded at 500 and 125 MHz, respectively. The FT-IR spectra of the samples as either neat or thin film were recorded using a PerkinElmer Spectrum Two spectrometer. All the samples were recorded using "attenuated total reflectance" (ATR) mode. The PIKE MIRacle single reflection horizontal ATR accessory equipped with a ZnSe ATR crystal was used for recording the spectra. The mass spectrometric data were obtained using a Micromass QuattroII, Micromass, triple quadrupole (LC-MS/MS) electrospray ionization mass spectrometer (ESI-MS) coupled with a Waters Agilent HPLC. We used a C18 column (2.1 × 30 mm) with flow rate of 0.45 mL min⁻¹. The mobile phase composition was a mixture of (A) water with 0.1% TFA and (B) acetonitrile with 0.1% TFA. The column temperature was maintained at 30 ± 1 °C. The gradient began at 95:5 of A:B with a flow of 0.2 mL/min. The gradient was changed to 5:95 of A:B over a course of 5 min followed by a 5 min hold at 5:95 of A:B. Over 0.1 min, the gradient was changed to 95:5 of

A:B with a concomitant change in flow rate to 0.45 mL/min. This was held for 0.8 min to complete the LC gradient (10 min total run time). The high resolution mass spectra (HRMS) were recorded on a Q-TOF mass spectrometer. The tensile and compression studies were performed using an H25KS UTM Tinius Olsen extensometer following the ASTM D638 protocol. The tensile or compression of samples were recorded as rectangular (width: 5 mm; thickness: 1 mm) or circular (radius: 18 mm; thickness: 5 mm) strips at ~25 °C using a 1.0 kN load cell and at a crosshead speed of 10.0 or 1.0 mm/min. The data represented here is an average of three specimens. The Young's moduli of the samples were determined from the linear region (Hookean slope) of the stress versus strain plot. Optical microscopic images of the samples were obtained at room temperature on a LEICA-DM750P instrument using a 10× or 40× objective. The dynamic mechanical analysis (DMA) was performed on a DMA Q-800 using the tension mode.⁵⁰ ASTM D4065-01 norm was followed to record the samples. The specimen samples of 5 mm width and 15 mm length were used for this purpose. The storage (G') and loss modulus (G'') data under variable frequency were recorded at constant oscillation amplitude (15 μ m). The complex modulus (G^*) was calculated using the formula

$$G^* = \sqrt{G'^2 + G''^2}$$

The differential scanning calorimetry (DSC) data of the samples were recorded on a DSC 25 TA Instruments under N₂ atmosphere (100 mL/min). Preweighted (3–9 mg) finely powdered samples were taken in an aluminum pan for the measurement. The samples were heated from –50 to 150 °C, cooled to –40 °C, and again heated to 140 °C at a rate of 10 °C/min. The data obtained from the second heating traces of the samples are reported in this article. Thermal gravimetric analysis (TGA) of the samples was recorded on a TGA Q500, TA Instruments under a N₂ atmosphere (60 mL/min). Approximately, 10 mg of finely powdered samples was taken in the platinum pan and heated up to 700 °C at a rate of 10 °C/min, and the weight loss was measured.

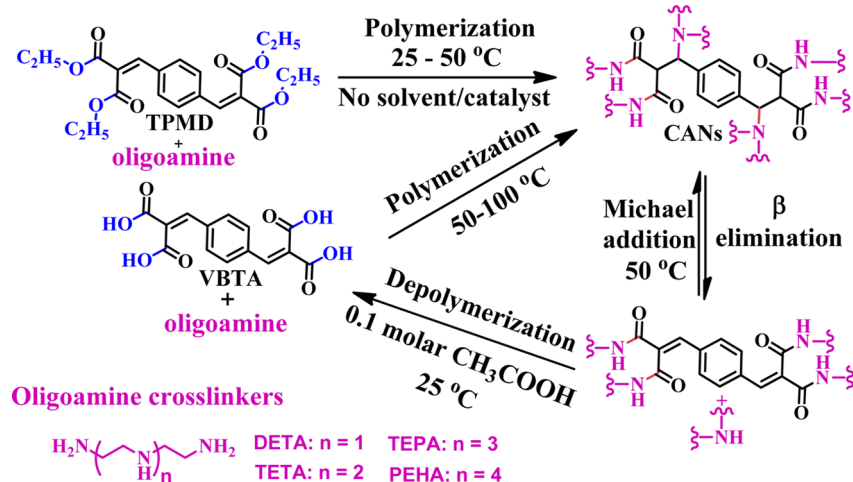
Synthesis of Tetraethyl-2,2'-[1,4-phenylenebis(methanyliidene)]dimalonate (TPMD). Terephthalaldehyde (3.0 g, 22.4 mmol) was dissolved in anhydrous ethanol (50 mL) in a round-bottom flask. To it DEM (8.9 g, 55.6 mmol) was added followed by piperidine (0.2 g, 2.3 mmol) and acetic acid (0.2 g, 3.3 mmol). The resulting mixture was refluxed overnight under an inert atmosphere. The temperature of the solution was then decreased to 25 °C, and the solvent was allowed to evaporate slowly to crystallize the product. The final product was obtained as white crystals (4.5 g, 10.8 mmol) in 48.2% yield. ¹H NMR (500 MHz, CDCl₃) δ (ppm): 7.62 (s, 2H, CH=C(COO)₂), 7.41 (s, 4H, ArH), 4.28 (q, 8H, –O–CH₂–), 1.25 (m, 12H, –O–CH₂–CH₃). ¹³C NMR (125 MHz, CDCl₃) δ (ppm): 164.5 (–COOCH₂), 142.7 (–CH=C–(COO)₂), 132.6 (Ar C), 130.1 (–CH=C–(COO)₂), 127.4 (Ar CH), 60.2 (–O–CH₂–), 14.0 (–O–CH₂–CH₃). FT-IR (thin film, cm⁻¹): 773 (m, *p*-substitution), 1200 (s, C–O), 1443 (m, C=C, Ar), 1488 (w, C–H), 1626 (m, C=C), 1719 (s, C=O), 2875 (w, C–H), 2976 (m, C–H). HRMS (ESI-TOF) *m/z*: [M + Na]⁺ Calcd for [C₂₂H₂₆O₈Na]⁺ 441.1525. Found 441.1523.

Preparation of TPMD-Based Networks. A typical procedure is described below. Synthesis of TPMD-TETA-3: TPMD (1.0 g, 2.4 mmol) and TETA (0.8 g, 5.6 mmol) were mixed together vigorously in a Teflon tray of circular cross section until a homogeneous solution obtained. The resulting solution was then kept undisturbed at 25 °C for 6 h to obtain a soft film. The film was then kept at 50 °C for 10 h to obtain the final network. FT-IR (thin film, cm⁻¹): 3287 (s, N–H), 2928 (m, C–H, Ar), 2853 (s, C–H, alkyl), 1641 (s, C=O, amide), 1559 (s, N–H), 1030 (s, C–N, amide), 1017 (s, C–N, Michael adduct), 818 (m, C–C, alkyl chain).

Similarly, four sets of networks were prepared by mixing TPMD and DETA, TETA, PEHA, or TEPA in different molar proportions and keeping the mixture at 25 °C for 6 h followed by heating the same at 50 °C for 10 h.

Recycling of Networks. A typical recycling procedure is described below; each film weighing ~5 g was cut into small pieces and

Scheme 1. Synthetic Pathway Showing the Formation and Depolymerization of TPMD and Oligoamine Cross-Linker Based CANs



transferred to 120 mL of 0.1 M acetic acid (pH = 5.3). The mixture was ultrasonicated for 1.5 h to obtain a homogeneous solution. The pH of the solution was then neutralized to 7.0. The resulting solution was then poured to a Teflon Petri disc and kept at 100 °C for 12 h to simultaneously evaporate the solvent and initiate polymerization process. Final curing was done at 50 °C for an additional 12 h to obtain the final networks. FT-IR (thin film, cm^{-1}): 3396 (s, N-H), 2926 (m, C-H, Ar), 2851 (s, C-H, alkyl), 1642 (s, C=O, amide), 1443 (w, C-H), 1016 (s, C-N, amide), 951 (s, C-N, Michael adduct), 822 (m, C-C, alkyl chain).

Reaction of TPMD with *n*-Butylamine at 50 °C (P-12). TPMD (2.0 g, 4.8 mmol) was added to *n*-butylamine (3.5 g, 48.0 mmol) in a 15.0 mL vial equipped with a magnetic stirrer. Within 15 min, a homogeneous mixture formed, and the mixture was allowed to stir for 6 h at 50 °C. The temperature of the reaction mixture was then cooled to 25 °C. The product obtained was dissolved in chloroform and washed repeatedly with water. Finally, the organic solution was passed over Na_2SO_4 and evaporated under reduced pressure to obtain the product as a sticky liquid (yield: 95.0%). ^1H NMR (500 MHz, CDCl_3) δ (ppm): 8.25 (s, 4H, -CONH-), 7.75 (s, 4H, ArH), 4.12 (m, 2H, -CH-CH-(CONH-)₂), 3.55 (m, 4H, -CH-NH-CH₂CH₂), 3.20 (m, 10H, -CONH-CH₂- and CH(CO)₂), 3.10 (s, 2H, -NH-CH₂-), 1.60 (m, 8H, -CONH-CH₂-CH₂) 1.35 (m, 4H, CHNH-CH₂CH₂), 1.25 (m, 4H, CHNHCH₂CH₂CH₂), 1.15 (m, 8H, CONHCH₂CH₂CH₂), 0.80 (m, 18H, -CH₃). ^{13}C NMR (125 MHz, CDCl_3) δ (ppm): 159.8 (-CONH), 137.5 (Ar C), 127.6 (Ar C), 61.0 (NH-CH-Ar), 59.9 (CH(CO)₂), 41.1 (CH-NH-CH₂) 32.4 (CONH-CH₂), 19.9 (NHCH₂-CH₂), 13.3 and 13.5 (-CH₂-CH₂-CH₃). FT-IR (neat, cm^{-1}): 3288 (s, C-H, alkyl), 2959 (s, C-H, Ar), 2931 (s, C-H, alkyl), 1644 (s, C=O, amide), 1542 (s, N-H, amide), 1464 (m, C-H), 1093 (m, C-N), 1050 (m, C-N). ESI-MS: m/z Calcd for $[\text{C}_{38}\text{H}_{67}\text{N}_6\text{O}_4\text{Na}_2]^+$ $[\text{M} + 2\text{Na} - \text{H}]^+$ 717.5. Found 717.5. HRMS (ESI-TOF) m/z : $[\text{M} + \text{Na}]^+$ Calcd for $\text{C}_{38}\text{H}_{68}\text{O}_4\text{N}_6\text{Na}$ 695.5200. Found 695.5203.

Reaction of TPMD with *n*-Butylamine at 10 °C (P-11). TPMD (2.0 g, 4.8 mmol) was added to *n*-butylamine (1.4 g, 19.2 mmol) in a 15.0 mL vial equipped with a magnetic stirrer at 10 °C. The mixture was stirred at 10 °C for 6 h. The product was then dissolved in chloroform and washed repeatedly with water to remove the unreacted starting material. Finally, the organic solution was passed over Na_2SO_4 and evaporated under reduced pressure to obtain the final product as a free-flowing liquid (yield: 92.0%). ^1H NMR (500 MHz, CDCl_3) δ (ppm): 8.25 (s, 4H, -CONH-), 7.72 (s, 4H, ArH), 7.45 (s, 2H, -CH=C-(CONH-)₂), 3.21 (m, 8H, -CONH-CH₂-), 1.48 (m, 8H, -CONH-CH₂-CH₂), 1.30 (m, 8H, -CH₂-CH₃), 0.82 (m, 12H, -CH₃). FT-IR (neat, cm^{-1}): 3316 (s, C-H, alkyl), 2959 (s, C-

H, Ar), 2931 (s, C-H, alkyl), 1644 (s, C=O, amide), 1539 (w, N-H, amide), 1465 (m, C-H), 1035 (s, C-N), 835 (w, C-C).

Degradation of P-12 in Acidic (pH = 5.3) Solution (P-13). The degradation procedure is described below; P-12 (1.0 g, 1.5 mmol) was transferred into a 15.0 mL vial containing 10 mL of 0.1 M acetic acid solution and mixed thoroughly. The milky solution became homogeneous after ultrasonication of the mixture for 1.5 h at 25 °C. The solution was then kept undisturbed at 25 °C for 24 h. White crystalline solids settled at the bottom was filtered and dried under vacuum (yield: 85.0%). ^1H NMR (500 MHz, CDCl_3) δ (ppm): 10.0 (s, 4H, -COOH), 7.0 (s, 4H, Ar-H), 4.25 (m, 2H, -NHCHC-HCOOH), 3.55 (m, 2H, -NHCHCHCOOH), 3.20 (m, 4H -NHCH₂-), 3.15 (s, 2H, -NHCH₂-), 1.40 (m, 4H, -NHCH₂CH₂-), 1.26 (m, 4H, -CH₂CH₃), 0.83 (m, 6H, -CH₃). ^{13}C NMR (125 MHz, CDCl_3) δ (ppm): 167.6 (C=O), 129.9 (Ar C), 128.2 (Ar CH), 60.5 (NHCHCH-), 43.0 (-NHCHCH-), 39.3 (-NHCH₂-), 31.3 (-NHCH₂CH₂-), 20.0 (-CH₂CH₂CH₃), 13.7 (-CH₂CH₃). FT-IR (neat, cm^{-1}): 3288 (s, O-H acid), 2959 (m, C-H, Ar), 2933 (m, C-H, alkyl), 1687 (m, C=O, acid), 1197 (s, -C-O, acid), 990 (m, C-N). ESI-MS: m/z Calcd for $[\text{C}_{22}\text{H}_{33}\text{N}_2\text{O}_8\text{Na}]^+$ $[\text{M} + \text{Na}]^+$ 475.2. Found 475.2. HRMS (ESI-TOF) m/z : $[\text{M} + \text{K} + \text{H}]^{2+}$ Calcd for $\text{C}_{22}\text{H}_{33}\text{O}_8\text{N}_2\text{K}$ 246.0937. Found 246.0936.

Reaction of TPMD with Diethylamine (P-21). TPMD (2.0 g, 4.8 mmol) was added to diethylamine (2.1 g, 28.7 mmol) in a 15.0 mL vial equipped with a magnetic stirrer. The mixture was stirred for 6 h at 50 °C. The temperature of the reaction mixture was then cooled to 25 °C. The resulting yellowish liquid was finally dried under vacuum (yield 85.0%).

Mono Aza-Michael Adduct. ^1H NMR (500 MHz, CDCl_3) δ (ppm): 7.62 (s, 1H, CH=C(COO)₂), 7.35 (d, 2H, Ar H), 7.15 (d, 2H, Ar H), 4.52 (m, 1H, CH-CH(COO)₂), 4.31 (m, 4H, -O-CH₂-), 4.23 (m, 4H, -O-CH₂-), 3.85 (m, 1H, CH-CH(COO)₂), 2.61 (m, 4H, -N-CH₂-CH₃), 1.25 (m, 12 H, -O-CH₂-CH₃), 0.80 (m, 6H, -N-CH₂-CH₃). ^{13}C NMR (125 MHz, CDCl_3) δ (ppm): 166.6 (COOCH₂), 137.3 (Ar C), 127.8 (Ar, CH), 62.2 (N-CH-Ar), 60.9 (O-CH₂), 55.2 (CH(CO)₂), 43.1 (N-CH₂), 13.2 (-CH₃). ESI-MS: m/z Calcd for $[\text{C}_{26}\text{H}_{38}\text{NO}_8]^+$ $[\text{M} + \text{H}]^+$ 492.3. Found 492.3. HRMS (ESI-TOF) m/z : $[\text{M} + \text{H}]^+$ Calcd for $\text{C}_{26}\text{H}_{38}\text{NO}_8$ 492.2597. Found 492.2552.

Bis Aza-Michael Adduct. ^1H NMR (500 MHz, CDCl_3) δ (ppm): 7.06 (s, 4H, ArH), 4.52 (m, 2H, CH-CH(COO)₂), 4.23 (m, 8H, -O-CH₂-), 3.85 (m, 2H, CH-CH(COO)₂), 2.61 (m, 8H, -N-CH₂-CH₃), 1.25 (m, 12 H, -O-CH₂-CH₃), 0.80 (m, 12H, -N-CH₂-CH₃). ^{13}C NMR (125 MHz, CDCl_3) δ (ppm): 167.3 (CH-CO-), 165.1 (=C-CO-), 140.9 (CH=C(CO)₂), 139.9 (Ar C), 133.6 (Ar C), 131.8 (Ar CH), 128.8 (Ar CH), 62.5 (N-CH-Ar), 60.9 (O-CH₂), 43.5 (N-CH₂), 13.3 (CH₂CH₃). ESI-MS: m/z Calcd for

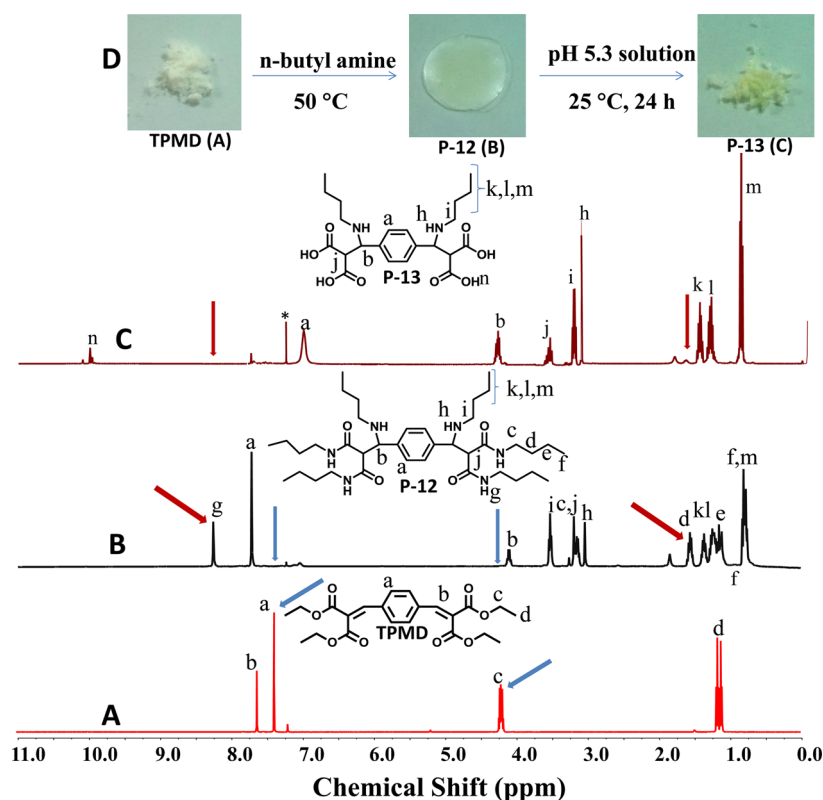


Figure 1. ^1H NMR spectra of (A) TPMD, (B) P-12, and (C) P-13. (D) Photographs of TPMD, P-12, and P-13. The peak marked with an asterisk is assigned to the CDCl_3 solvent.

$[\text{C}_{30}\text{H}_{49}\text{N}_2\text{O}_8]^+ [\text{M} + \text{H}]^+ 565.3$. Found 565.3. HRMS (ESI-TOF) m/z : $[\text{M} + \text{H}]^+$ Calcd for $\text{C}_{30}\text{H}_{49}\text{N}_2\text{O}_8$ 565.3489. Found 565.3483. FT-IR (neat, cm^{-1}): 2980 (s, C–H, Ar), 2890 (m, C–H, alkyl), 1730 (s, C=O, ester), 1646 (m, C=C), 1464 (m, C–H, alkyl), 1253 (s, C–O, ester) 1035 (s, C–N), 857 (w, C–C).

Degradation of P-21 at 25 °C. The liquid P-21 (1.0 g) was kept in an open sample vial at 25 °C for 48 h. The physical state of the compound changed to solid. ^1H NMR (500 MHz, CDCl_3) δ (ppm): 7.65 (s, 2H, $\text{CH}=\text{C}(\text{COO})_2$), 7.49 (s, 4H, Ar H), 4.28 (q, 8H, $-\text{O}-\text{CH}_2-$), 1.65 (m, 12H, $-\text{O}-\text{CH}_2-\text{CH}_3$). ^{13}C NMR (125 MHz, CDCl_3) δ (ppm): 163.2 ($-\text{COOCH}_2$), 140.1 ($\text{CH}=\text{C}(\text{COO})_2$), 133.8 ($\text{CH}=\text{C}(\text{COO})_2$), 128.6 (Ar CH), 124.4 (Ar C), 60.2 ($-\text{O}-\text{CH}_2-$), 12.8 ($-\text{O}-\text{CH}_2-\text{CH}_3$). FT-IR (neat, cm^{-1}): 2980 (m, C–H), 2876 (w, C–H), 1719 (s, C=O), 1626 (m, C=C), 1488 (w, C–H), 1443 (m, C=C, Ar), 1200 (s, C–O), 773 (m, *p*-substitution). ESI-MS: m/z calcd for $[\text{C}_{22}\text{H}_{25}\text{O}_8\text{Na}_2]^+ [\text{M} + 2\text{Na}-\text{H}]^+$: 463.2. Found: 463.2. HRMS (ESI-TOF) m/z : $[\text{M} + \text{Na}]^+$ Calcd for $[\text{C}_{22}\text{H}_{26}\text{O}_8\text{Na}]^+$ 441.1525. Found 441.1526.

Determination of Gel Fraction. A typical procedure is described below. A thin piece of CAN (150–300 mg) was dipped in methanol (10 mL) and left undisturbed for 18 h at 25 °C. The solvent was then replaced with 10 mL of fresh methanol. After 8 h, the same process was repeated for one more cycle. Finally, the solvent was decanted off, and the sample was dried under vacuum and the weight of resulting sample was recorded. The gel fraction was determined by the equation

$$\text{gel fraction} = (W_f/W_i) \times 100$$

where W_f and W_i are the final and initial weights of the sample, respectively.

Gel fractions of TPMD-DETA-3, TPMD-TETA-3, TPMD-TEPA-3, and TPMD-PEHA-3 were determined to be 97.7, 97.5, 98.0, and 98.3%, respectively.

RESULTS AND DISCUSSION

TPMD was synthesized using a procedure similar to that of the reported in the literature.⁵¹ TPMD and commercially available oligoamines $[\text{NH}_2(\text{C}_2\text{H}_4\text{NH})_n\text{C}_2\text{H}_4\text{NH}_2$, $n = 1-4$] possessing primary (1°) and secondary (2°) amine functionalities were cross-linked under mild temperature (25–50 °C) conditions to synthesize the networks through possible formation of amide linkage and aza-Michael adduct (Scheme 1). No solvent or catalyst was used in the preparation step. Bands at 1719 (C=O) and 1200 cm^{-1} (C–O) assigned to the $-\text{COOC}_2\text{H}_5$ of TPMD disappeared, and new bands at 1641 (C=O) and 1030 cm^{-1} (C–N) appeared in the FTIR spectrum of the resulting network supporting the formation of amide linkage (Supporting Information, Figure S1). The 1° amines are known to react with carboxylate moieties possessing activating groups at the α carbon under ambient conditions to form the corresponding amides.^{52,53} Similarly, the disappearance of band at 1626 cm^{-1} (C=C of TPMD) and appearance of band at 1017 cm^{-1} (C–N) suggested the formation of aza-Michael adducts in the network (Figure S1). Though a catalyst is typically used in the literature for the aza-Michael addition,⁵⁴ in this particular case the reaction progressed under catalyst free conditions possibly due to involvement of highly conjugated double bond as the Michael acceptor.⁴⁸

To gain further insight into the polymerization pathways of CANs, suitable model compounds were synthesized under the polymerization conditions by reacting TPMD with 1° and 2° amine. Keeping the steric suitability of oligoamine cross-linkers in mind, *n*-butylamine and diethylamine were chosen as the 1° and 2° amine, respectively. The reactions were carried out under both low (10 °C) and moderate (50 °C) temperature conditions. Both aza-Michael addition and amidation between

1° amine (*n*-butyl amine) and TPMD proceeded to completion under solvent-free conditions at 50 °C. In ¹H NMR spectra, resonance at 4.28 ppm assigned to the $-\text{COOCH}_2-$ of TPMD disappeared, and new resonances at 8.25, 3.20, and 1.60 ppm accountable to $-\text{CONHCH}_2-$, $-\text{CONHCH}_2-$, and $-\text{CONHCH}_2\text{CH}_2-$, respectively, appeared, suggesting quantitative amidation of TPMD (P-12) (Figures 1A,B). Similarly, the disappearance of resonance at 7.62 ppm accountable to $\text{Ph}-\text{CH}=\text{C}(\text{CO})_2-$ and appearance of peaks at 4.12 and 3.55 ppm for $-\text{NHCHCH}(\text{CO})_2-$ and $-\text{CHNHCH}_2-$, respectively, suggested successful aza-Michael addition between *n*-butylamine and TPMD double bonds. The aromatic peak at 7.41 ppm also shifted to 7.75 ppm, suggesting the formation of overall product. The peak at 164.5 ppm shifted to 159.8 ppm and the resonances at 142.7 and 130.1 ppm disappeared in the ¹³C NMR spectrum of P-12, supporting amidation of the ester functionality and aza-Michael addition of amine functionality to the α,β -unsaturated double bond, respectively (Figure S2A). The FTIR bands at 1719 (C=O) and 1200 cm^{-1} (C–O) for the carboxylate group disappeared, and new bands at 1644 (C=O) and 1050 cm^{-1} (C–N) accountable to amide linkage appeared suggesting formation of the product (P-12) (Figures 2A,B). The peak for P-12 $[\text{M} + 2\text{Na}-\text{H}]^+$ was visible at 717.5

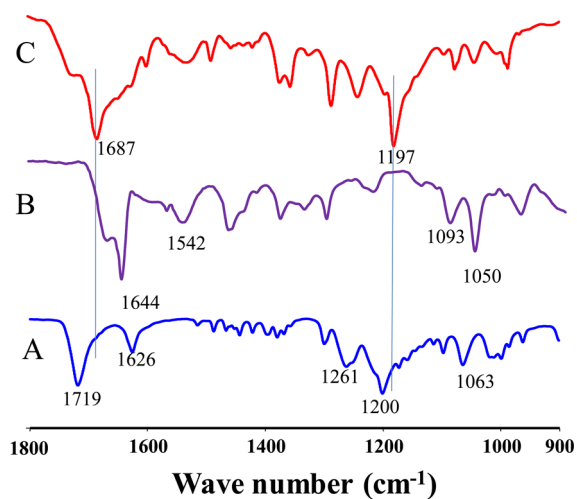


Figure 2. FT-IR spectra of (A) TPMD, (B) product (P-12) of reaction between TPMD and *n*-butylamine at 50 °C, and (C) P-13 (hydrolyzed product of P-12).

in the ESI-MS spectrum (Figure S3). The HRMS peak at 695.5203 accountable to the $[\text{M} + \text{Na}]^+$ supported the formation of P-12. TPMD, a white crystalline solid at 25 °C, changed to viscous liquid after reaction with *n*-butylamine at 50 °C (Figure 1D). At low temperature (10 °C), amidation between *n*-butylamine and TPMD prevailed over aza-Michael addition. The peaks at 4.28 and 1.25 ppm accountable to $-\text{OCH}_2-$ and $-\text{OCH}_2\text{CH}_3$, respectively, in TPMD disappeared, and new resonances at 3.21, 1.48, and 0.82 ppm accountable to $-\text{CONHCH}_2-$, $-\text{CONHCH}_2\text{CH}_2-$, and $-\text{CH}_2\text{CH}_3$, respectively, appeared in the ¹H NMR spectra of the product, suggesting quantitative amidation (Figure S4B). However, the presence of small resonances at 3.62 and 1.58 ppm suggested formation of a small amount of aza-Michael adduct along with P-11. The resulting product was a free-flowing colorless liquid.

No reaction between 2° amine (diethylamine) and TPMD was witnessed at low and ambient conditions (temperature ≤ 25 °C). At higher temperature (50 °C), the reaction between TPMD and diethylamine was restricted to the formation of aza-Michael adduct only. ¹H NMR spectroscopic analysis revealed the presence of both mono and bis aza-Michael adduct along with a trace amount of TPMD and existence of a dynamic equilibrium between Michael addition and β elimination. In the aromatic region, resonances at 7.06 ppm (bis aza-Michael adduct), 7.15 and 7.35 ppm (mono aza-Michael adduct), and 7.41 ppm (TPMD) were visible (inset, Figure 3B). The integration of the above peaks revealed that the mono and bis aza-Michael adducts and TPMD are present in 69:21:10 molar ratio in the product. New resonances at 3.85 and 4.52 ppm accountable to $-\text{CH}-\text{CH}(\text{CO})_2$ and $(\text{C}_2\text{H}_5)_3\text{N}-\text{CH}-$ supported the formation of above aza-Michael adducts. The ¹³C NMR spectrum of P-21 showed the characteristic resonances for both mono and bis aza-Michael adducts along with the precursor (Figure S2B). The FTIR band at 1719 cm^{-1} (C=O) assigned to the COOC_2H_5 in TPMD shifted to higher frequency (1730 cm^{-1}) region, suggesting loss of conjugation due to the formation of the aza-Michael adduct (Figure S5B). The intensity of band at 1626 cm^{-1} (C=C) substantially decreased in the product. The mono ($[\text{M} + \text{H}]^+$: 492.3) and bis ($[\text{M} + \text{H}]^+$: 565.3) aza-Michael adducts were also detected in ESI-MS analysis (Figure S6). The HRMS data further supported the product formation by displaying peaks at 492.2552 ($[\text{M} + \text{H}]^+$ of mono adduct) and 565.3483 ($[\text{M} + \text{H}]^+$ of bis adduct). On exposing the above product (P-21) to atmospheric conditions (25 °C), β elimination readily occurred and TPMD was isolated after 48 h. Gradual evaporation of volatile diethylamine (boiling point: 55 °C) under ambient condition also favored the β elimination by shifting the equilibrium toward reverse direction. The ¹H NMR spectrum of the compound obtained after storing P-21 at 25 °C for 48 h matched with that of the TPMD, suggesting quantitative recovery of the precursor (Figures 3A,C). The FTIR bands at 1626 and 1719 cm^{-1} accountable to TPMD reappeared supporting the above (Figure S5C). ESI-MS spectra of the aged P-21 after 48 h of storage displayed the peak for TPMD ($[\text{M} + 2\text{Na}-\text{H}]^+$: 463.2) (Figure S7). The physical state of TPMD also notably changed from solid to liquid after reaction with diethylamine (Figure 3D). The state again changed back to solid on exposing P-21 to the atmosphere for 48 h. However, no trace of amidation between diethylamine and TPMD was noticed up to 12 h of reaction time at 50 °C. The resistance of diethylamine toward amidation is attributed to the steric hindrance around the $-\text{NH}-$ moiety offered by two N-ethyl groups.

The degradability of the amide linkage in acidic solution was studied by adding P-12 to pH 5.3 aqueous solution at 25 °C. The milky solution became homogeneous after 1.5 h of ultrasonication, suggesting possible degradation of the amide linkage (Figure S8B). White crystalline solids settled at the bottom on keeping the above homogeneous solution undisturbed for 24 h at 25 °C. The ¹H NMR spectrum of the above crystalline solid showed appearance of resonance at 10.0 ppm accountable to $-\text{COOH}$, disappearance of resonance at 8.25 ppm assigned to $-\text{CONH}-$, and upfield shifting of aromatic resonance from 7.75 to 7.0 ppm, suggesting formation of the corresponding tetracarboxylic acid (P-13). All the proton resonances assigned to $-\text{CONHCH}_2\text{CH}_2\text{CH}_2\text{CH}_3$ disappeared in the degraded product supporting successful cleavage of the

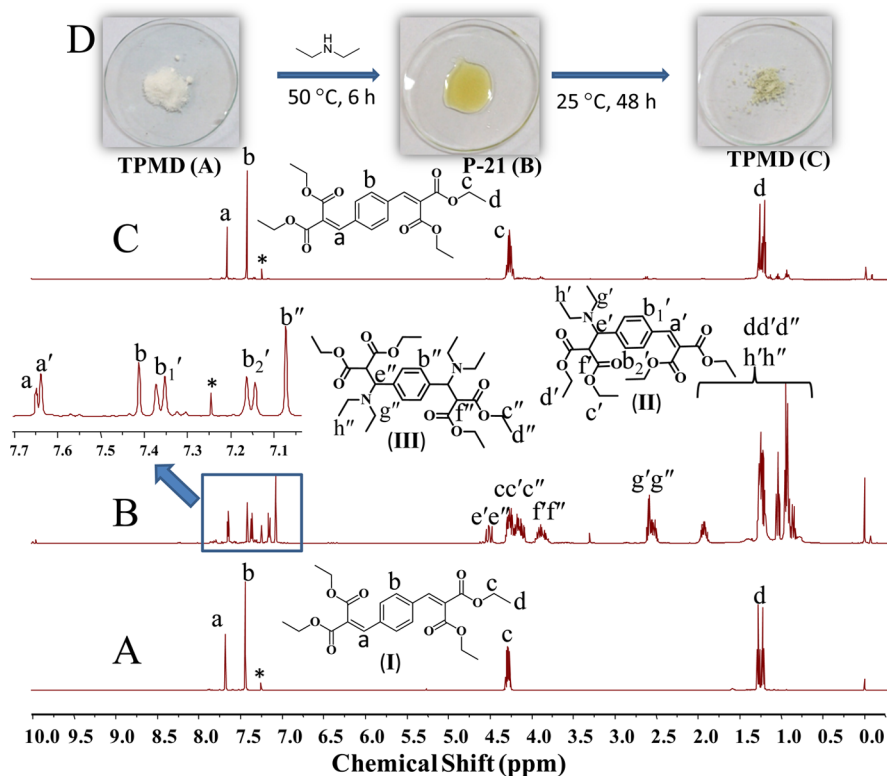
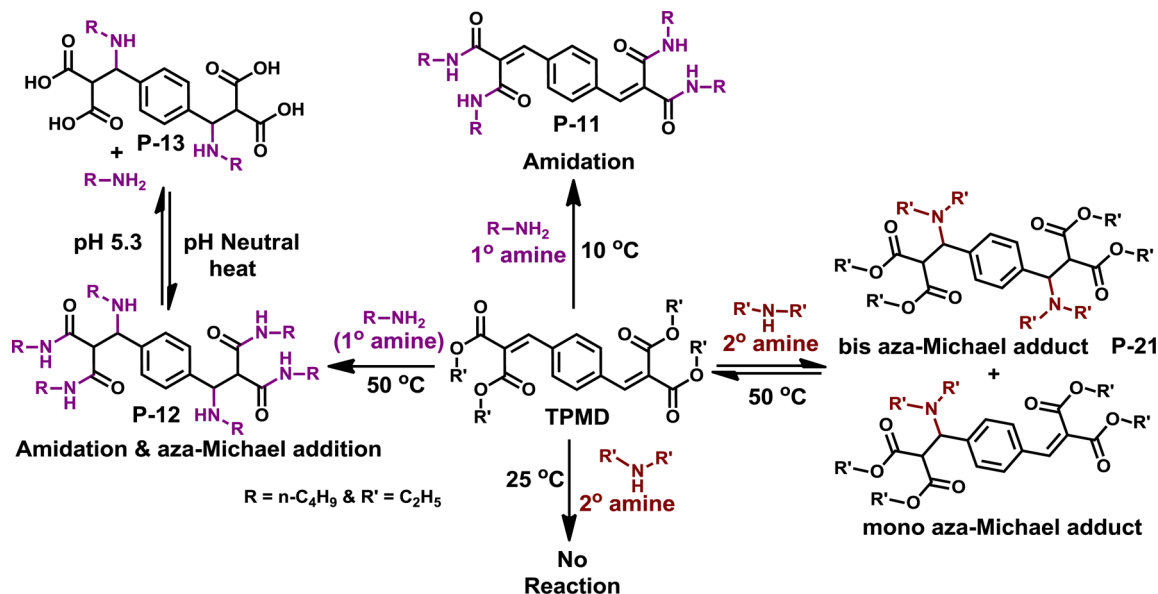


Figure 3. ^1H NMR spectra of (A) TPMD, (B) P-21 (mixture of TPMD (I), mono (II), and bis (III) aza-Michael adduct), (C) the product obtained after exposing P-21 to the atmosphere for 48 h, and (D) photographs of TPMD, P-21, and aged P-21 after 48 h. The peaks marked with an asterisk represents CDCl_3 solvent.

Scheme 2. Reactivity of TPMD toward 1° (*n*-Butylamine) or 2° (Diethylamine) Amine under Different Conditions



amide linkage (Figure 1C). The appearance of new FTIR bands at 1687 ($\text{C}=\text{O}$) and 1197 cm^{-1} ($\text{C}-\text{O}$) for the COOH functionality supported successful hydrolysis of amide functionalities and formation of P-13 (Figure 2C). The ESI-MS trace displayed the characteristic peak for P-13 ($[\text{M} + \text{Na}]^+$: 475.2) (Figure S9).

On the basis of above information, the following pathway for the reactions between TPMD and 1° or 2° amines is proposed (Scheme 2).

With 1° amine ($-\text{NH}_2$), amidation preferably occurs at low temperature (10°C), whereas at moderate temperature (50°C) both Michael addition and amidation proceed to completion. The amide linkage formed with 1° amine is easily hydrolyzable in acidic ($\text{pH} \leq 5.3$) medium. The 2° amine ($-\text{NH}-$) is not capable of forming amide linkage under polymerization conditions and forms a reversible aza-Michael adduct with TPMD. The above fully supported the polymer-

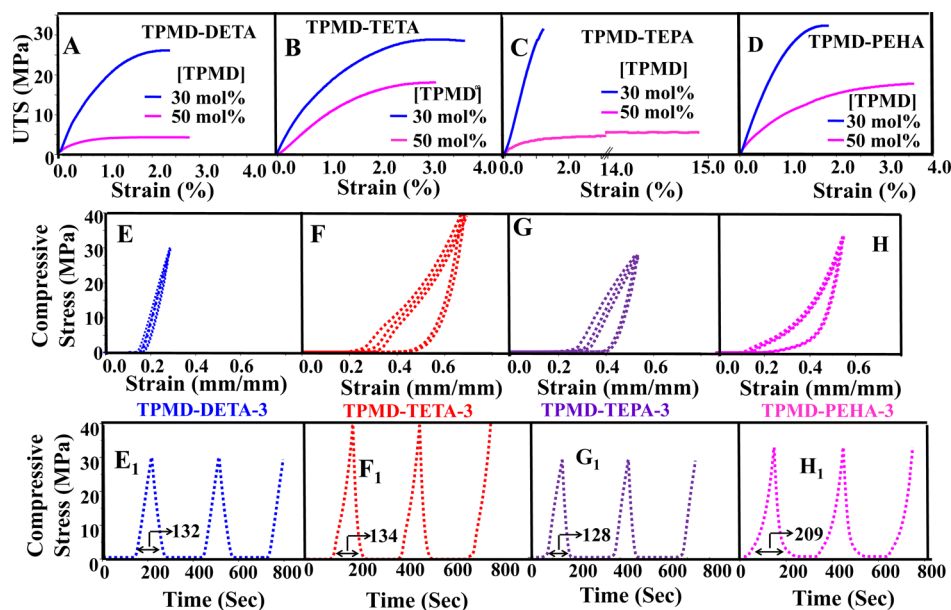


Figure 4. (A–D) Tensile plots of the CANs, (E–H) hysteresis curves from uniaxial compression tests, and (E1–H1) compressive stress versus time profiles of the CANs ([TPMD] \approx 30 mol %) for three load–unload cycles.

ization/depolymerization pathway for the networks proposed in Scheme 1.

The as-synthesized thin films of the networks were uniform and displayed a characteristic color based on the type and amount of oligoamine cross-linker in the networks (Figure S10). Since the cross-linking was carried out under solvent-free condition, the mol % of TPMD in the networks was restricted between 30 and 50.⁵⁵ The CANs exhibited adequate solvent resistance and swelled marginally (<10% of the initial weight after 12 h) in few high polarity solvents such as methanol and NMP (Figure S11). The gel fractions of the CANs possessing 30 mol % of TPMD were determined using methanol as the solvent and found to be in the range of 97–98%.

The networks possessing 30 mol % of TPMD (functional group equivalence of COOC_2H_5 to $\text{NH}_2 \approx 1:1$) exhibited optimum ultimate tensile strength (UTS) (23–35 MPa) and Young's modulus (1.9–3.0 GPa) (Figures 4A–D and Table S1). The modulus is comparable to several commercial polyamides and other high strength polymers.⁵⁶ The G^* (4.5–7.9 GPa at 1 Hz) values obtained from the DMA analysis also supported the Young's modulus values and stiffness of the networks (Figure 5). The G' values were higher than G'' values throughout the frequency range, suggesting cross-linked nature of the samples. On changing the mol % of TPMD to 50 (functional group equivalence of COOC_2H_5 to $\text{NH}_2 \approx 2:1$), the UTS (3.6–21.9 MPa) and modulus (0.2–1.7 GPa) decreased due to a possible decrease in degree of cross-linking. For a fixed TPMD:cross-linker (30:70, mol:mol) ratio, the UTS and Young's modulus of the networks gradually increased with the increase in number of $-\text{NH}-$ (2° amine) groups in the cross-linker (Figure 6A). The network based on DETA (one $-\text{NH}-$ group) exhibited least UTS (22.8 MPa) and modulus (2.0 GPa), whereas the UTS and modulus of the network based on PEHA (four $-\text{NH}-$ groups) increased up to 30.9 MPa and 3.0 GPa, respectively. The G^* values also gradually increased with the increase in number of $-\text{NH}-$ in the cross-linker (Figure 5). Since $-\text{NH}-$ is not capable of forming amide bond with TPMD under polymerization conditions, the above increase in stiffness could be attributed to the additional

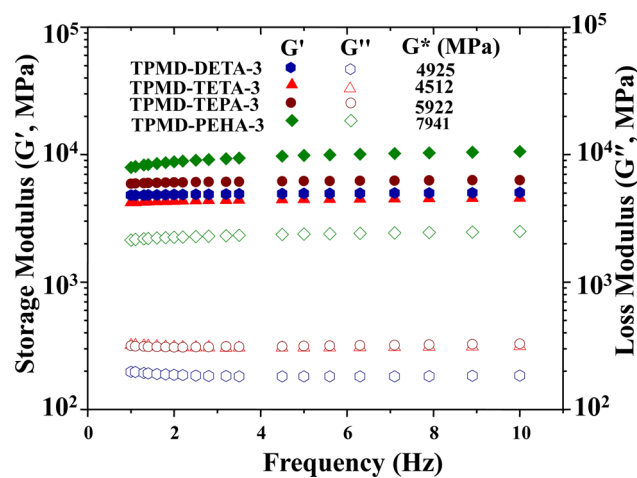


Figure 5. DMA (G'/G'' versus frequency) data of the CANs recorded at 25 °C.

cross-linking resulting from the formation of aza-Michael adducts in the samples.

To understand the performance of these networks under load, hysteresis studies under compression were carried out with networks possessing 30 mol % of TPMD. The CANs endured compressive stress up to 30 MPa. The nature of the loading curve was similar to that of the reported network based on amide linkage.⁵⁷ The networks displayed typical viscoelastic behavior with noticeable hysteresis during the repetitive cycles (Figures 4E–H). Importantly, the samples quantitatively recovered from stress for all three cyclic measurements, and no residual strain was noticed after each cycle. The unloading curves of the cycles superimposed upon each other in the case of all the samples. The area within the hysteresis loop reflected the amount of energy dissipated during the load–unload cycles. The energy dissipation per unit volume of DETA based network (0.6 MJ/m³) was 1 order of magnitude lower compared to those of the other networks (2.4–4.9 MJ/m³) (Figure 6B).

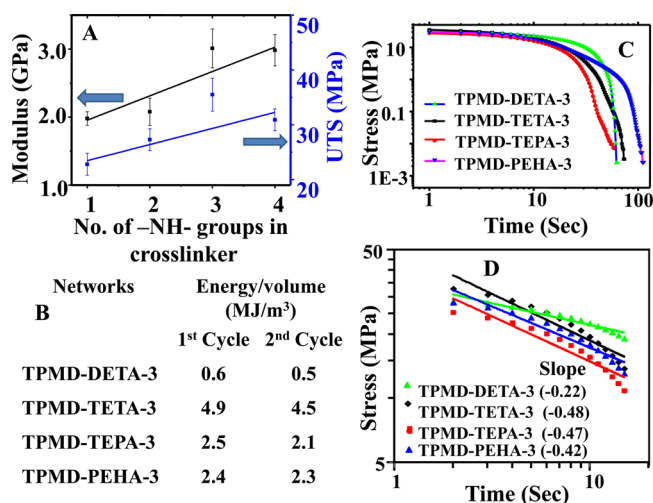


Figure 6. (A) Variation in modulus and UTS of the networks with the number of 2° amine (–NH–) groups in the cross-linker; the networks studied have 30 mol % of TPMD. (B) Energy loss per unit volume data derived from the area of hysteresis loops. (C) Stress versus time plots of the networks derived from a typical decompression curve of the first cycle (the data from the first cycles of each network is adopted from Figures 4E1–H1 for this purpose). (D) Magnified view of the plateau region (for time scale in the range of 1–15 s) in (B).

The compressive stress versus time profiles of the networks for continuous three cycles are shown in Figures 4E1–H1. Typical compression and release cycles were recorded between 128 and 209 s at 1 mm/min scan rate. The stress versus time plots derived from the decompression curves of the first cycle revealed a plateau region up to initial 10 s and an exponential decay afterward (Figure 6C). The terminal behavior of TPMD-DETA-3 showed a much faster decay (time constant ~ 1.4 s) compared to those of the networks based on the other cross-linkers (time constants $\approx 6.2 \pm 0.9$ s).⁵⁸ The slopes of the plateau regions (0.42–0.48) suggested that the network strands in TETA-, TEPA-, and PEHA-based systems followed a Rouse-like dynamics with a relaxation time of ~ 10 s, whereas the DETA-based system exhibited a much smaller slope (0.22) (Figure 6D). This suggested the DETA-based network has a more compact structure and incurs less viscous loss during the stress loading–relaxation cycles compared to the others.⁵⁹

The DSC analysis of the CANs possessing 30 mol % of TPMD and different oligoamine cross-linkers was conducted under a N₂ atmosphere. As anticipated, no noticeable thermal transition occurred in the temperature range of -35 to 140 °C owing to the cross-linked nature of the samples (Figure S12). The TGA data of the CANs possessing 30 mol % TPMD were recorded under a N₂ atmosphere in the temperature range of 20 – 700 °C (Figure 7). The initial minor weight loss ($\leq 5\%$) in the range of 20 – 70 °C could be attributed to the presence of moisture and other volatile impurities in the samples. These CANs exhibited thermal stability up to ~ 220 °C. The first considerable weight loss (12–30%) occurred in the range of 230 – 280 °C. The subsequent and maximum weight loss (23–36%) was witnessed in the temperature range of 300 – 440 °C. Conventional aliphatic polyamides are known to possess high thermal stability up to 350 °C and low char yield ($< 5\%$).⁶⁰ The lower thermal stability of these networks compared to that of the conventional polyamide could be attributed to the presence of aliphatic malonamide moiety in the structure. Aliphatic polymalonamides are known to possess moderate thermal stability

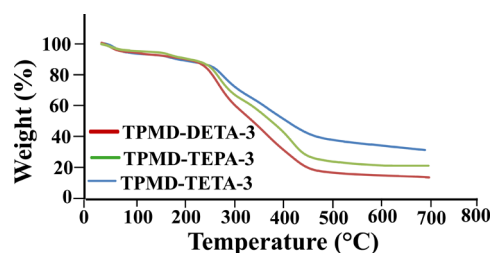


Figure 7. TGA traces of CANs possessing 30 mol % of TPMD and different oligoamine cross-linkers recorded under a N₂ atmosphere.

up to ~ 300 °C.⁶¹ Reasonably high char yields (18–38%) of the samples supported the cross-linked nature of these networks (Table S2).⁶²

To explore the recyclability of these networks, the effect of different pH conditions on their degradability was studied. Thin films of the networks were cut into small pieces and dipped in a particular pH solution. The films dipped in mildly acidic (pH = 5.3) solution dissolved after 1.5 h of ultrasonication at 25 °C, whereas no noticeable change to the samples occurred in neutral and basic (pH = 10.5) solutions up to 6 h (Figures 8C,E,F). In acidic solution, a possible depolymerization of the networks occurred through the hydrolysis of amide linkages (Scheme 1). To further understand the degradation pattern, the change in compressive modulus of the samples dipped in pH 5.3 solution was measured after a regular time period (Figure 8A). A substantial loss (70–100%) in compressive strength was observed in all the cases after 3 h of dipping time. The gradual loss in modulus with time revealed that the degradation occurred in bulk and was not restricted only to the surface of the films.

The recycling process of these networks is fairly simple. After dissolution of the network in acidic solution, the pH was neutralized to 7.0, and the temperature of the solution was raised to 100 °C to simultaneously evaporate the water and cross-link the resulting tetracarboxylic acid (VBTA) with amine functionality (Scheme 1). The appearance of peaks at 1643 (C=O) and 1551 cm⁻¹ (N–H) supported the formation of amide cross-links in the recycled networks (Figure S13). The condensation of carboxylic acid with 1° amine at 80 – 110 °C to form the amide under solvent-free conditions is reported in the literature.^{63,64} The re-formed networks exhibited comparable tensile properties to that of the parent networks, suggesting these samples could be recycled with retention of their mechanical properties (Figures 8G–J and Table S3).

Moreover, the thermoresponsiveness of the aza-Michael addition between 2° amine (–NH–) and activated double bond was utilized to achieve self-healing in the CANs. Thin slits made on the surface of the thin films were exposed to 50 °C. As shown in Figure 9, TPMD-DETA-3 quantitatively healed within 30 min, whereas a healing time of ~ 1 h was necessary to completely heal the TPMD-DETA-3 sample. Possibly, a higher number of –NH– groups present in PEHA (four) compared to that of the DETA (one) facilitated the aza-Michael addition and enhanced the rate of healing in the samples synthesized using the former as cross-linker.

In conclusion, dynamic amidation and aza-Michael addition chemistry could be utilized to develop recyclable and healable networks. These networks possess adequate strength and mechanical reversibility from stress, suggesting these could be used for various load bearing applications. The networks could be depolymerized in mild acidic solution and repolymerized

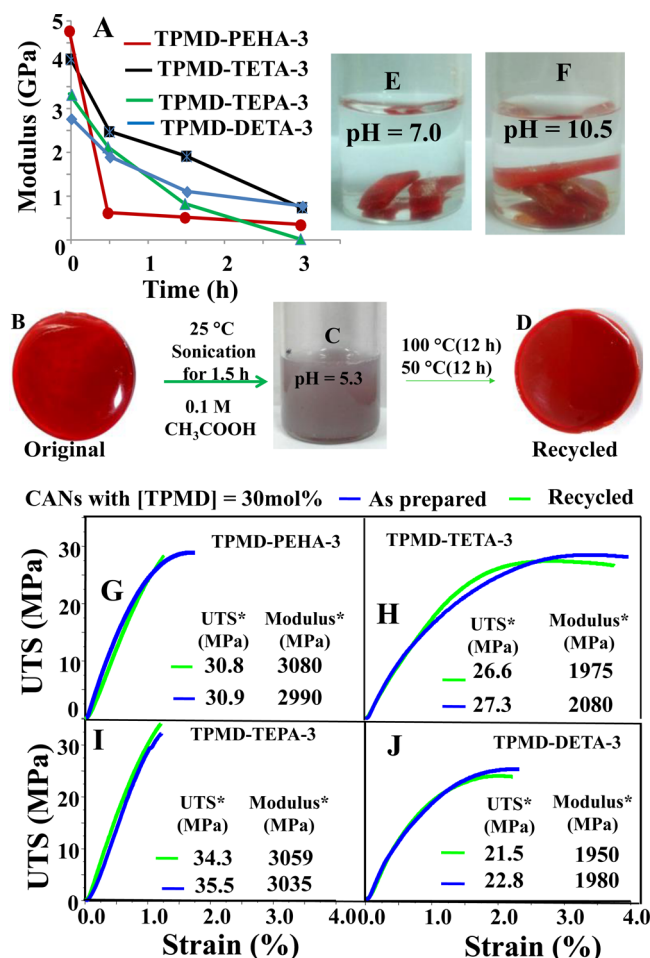


Figure 8. (A) Compressive modulus of the networks after different dipping time in acidic (pH = 5.3) solution. (B, D) Photographs of original and recycled TPMD-TETA-3 thin films ([TPMD] \approx 30 mol %) and (C, E, F) small pieces of TPMD-TETA-3 in different pH solutions. (G–J) Tensile plots of original and recycled networks. *The data is an average of at least three measurements.

without sacrificing mechanical properties. These networks are stable to various organic and aqueous environments. Cracks and defects on these material surfaces could be self-healed under moderate temperature conditions. These networks can be easily synthesized in a large scale under solvent-free and moderate temperature conditions. The facile synthesis, cost effectiveness, and recyclability render these networks suitable for a range of applications.

■ ASSOCIATED CONTENT

Supporting Information

The Supporting Information is available free of charge on the ACS Publications website at DOI: 10.1021/acs.macromol.6b01807.

Tables containing tensile and TGA data, photographs of the strips, FTIR spectra of the networks and model compounds, ^1H and ^{13}C NMR spectra and ESI-MS traces of model compounds, DSC traces, swelling ratios and photographs (PDF)

■ AUTHOR INFORMATION

Corresponding Author

*E-mail uojha@rgipt.ac.in, phone 05352704221 (U.O.).

Notes

The authors declare no competing financial interest.

■ ACKNOWLEDGMENTS

A.K. thanks CSIR, India, for the research fellowship. TA Instruments, Bengaluru, India, is acknowledged for the thermal analysis of the samples.

■ REFERENCES

- Barnes, D. K.; Galgani, F.; Thompson, R. C.; Barlaz, M. Accumulation and Fragmentation of Plastic Debris in Global Environments. *Philos. Trans. R. Soc., B* **2009**, *364*, 1985–1998.
- Rowan, S. J.; Cantrill, S. J.; Cousins, G. R. L.; Sanders, J. K. M.; Stoddart, J. F. Dynamic Covalent Chemistry. *Angew. Chem., Int. Ed.* **2002**, *41*, 898–952.

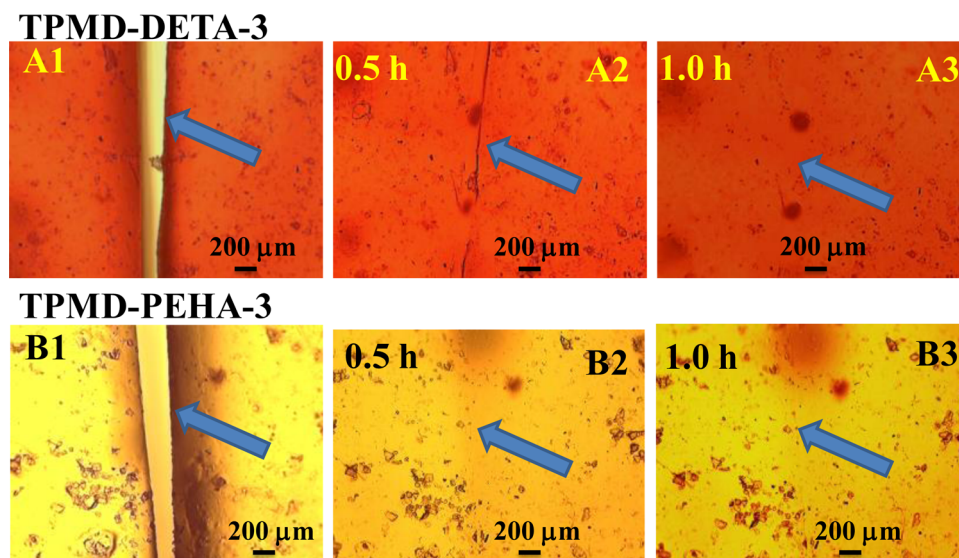


Figure 9. TPMD-DETA-3 and TPMD-PEHA-3 thin films with narrow slits (A1, B1), recovery after 0.5 h (A2, B2), and 1 h (A3, B3), respectively, at 50 °C.

- (3) Whitaker, D. E.; Mahon, C. S.; Fulton, D. A. Thermoresponsive Dynamic Covalent Single-Chain Polymer Nanoparticles Reversibly Transform into a Hydrogel. *Angew. Chem., Int. Ed.* **2013**, *52*, 956–959.
- (4) Lyon, G. B.; Baranek, A.; Bowman, C. N. Scaffolded Thermally Remendable Hybrid Polymer Networks. *Adv. Funct. Mater.* **2016**, *26*, 1477–1485.
- (5) Bowman, C. N.; Kloxin, C. J. Covalent Adaptable Networks: Reversible Bond Structures Incorporated in Polymer Networks. *Angew. Chem., Int. Ed.* **2012**, *51*, 4272–4274.
- (6) Kloxin, C. J.; Bowman, C. N. Covalent Adaptable Networks: Smart, Reconfigurable and Responsive Network Systems. *Chem. Soc. Rev.* **2013**, *42*, 7161–7173.
- (7) Habault, D.; Zhang, H.; Zhao, Y. Light-Triggered Self-Healing and Shape-Memory Polymers. *Chem. Soc. Rev.* **2013**, *42*, 7244–7256.
- (8) Urban, M. W. Dynamic materials: The Chemistry of Self-Healing. *Nat. Chem.* **2012**, *4*, 80–82.
- (9) Ying, H.; Zhang, Y.; Cheng, J. Dynamic Urea Bond for the Design of Reversible and Self-Healing Polymers. *Nat. Commun.* **2014**, *5*, 3218.
- (10) Neal, J. A.; Mozhdzhi, D.; Guan, Z. Enhancing Mechanical Performance of a Covalent Self-Healing Material by Sacrificial Noncovalent Bonds. *J. Am. Chem. Soc.* **2015**, *137*, 4846–4850.
- (11) Wojtecki, R. J.; Meador, M. A.; Rowan, S. J. Using the Dynamic Bond to Access Macroscopically Responsive Structurally Dynamic Polymers. *Nat. Mater.* **2011**, *10*, 14–27.
- (12) Lehn, J. M. Perspectives in Chemistry—Aspects of Adaptive Chemistry and Materials. *Angew. Chem., Int. Ed.* **2015**, *54*, 3276–3289.
- (13) Ciesielski, A.; El Garah, M.; Haar, S.; Kovaricek, P.; Lehn, J. M.; Samori, P. Dynamic Covalent Chemistry of Bisimines at the Solid/Liquid Interface Monitored by Scanning Tunneling Microscopy. *Nat. Chem.* **2014**, *6*, 1017–1027.
- (14) Kovaříček, P.; Lehn, J. M. Merging Constitutional and Motional Covalent Dynamics in Reversible Imine Formation and Exchange Processes. *J. Am. Chem. Soc.* **2012**, *134*, 9446–9455.
- (15) Fevre, M.; Jones, G. O.; Zhang, M.; García, J. M.; Hedrick, J. L. Melt-Processable Dynamic-Covalent Poly(hemiaminal) Organogels as Scaffolds for UV-Induced Polymerization. *Adv. Mater.* **2015**, *27*, 4714–4718.
- (16) Fox, C. H.; ter Hurne, G. M.; Wojtecki, R. J.; Jones, G. O.; Horn, H. W.; Meijer, E. W.; Frank, C. W.; Hedrick, J. L.; García, J. M. Supramolecular Motifs in Dynamic Covalent PEG-Hemiaminal Organogels. *Nat. Commun.* **2015**, *6*, 7417–7425.
- (17) Folmer-andersen, J. F.; Lehn, J. M. Constitutional Adaptation of Dynamic Polymers: Hydrophobically Driven Sequence Selection in Dynamic Covalent Polyacylhydrazones. *Angew. Chem., Int. Ed.* **2009**, *48*, 7664–7667.
- (18) Hirsch, A. K. H.; Buhler, E.; Lehn, J. M. Biodynamers: Self-Organization-Driven Formation of Doubly Dynamic Proteoids. *J. Am. Chem. Soc.* **2012**, *134*, 4177–4183.
- (19) Jackson, A. W.; Fulton, D. A. Dynamic Covalent Diblock Copolymers Prepared from RAFT Generated Aldehyde and Alkoxyamine End-Functionalized Polymers. *Macromolecules* **2010**, *43*, 1069–1075.
- (20) Mukherjee, S.; Hill, M. R.; Sumerlin, B. S. Self-Healing Hydrogels Containing Reversible Oxime Crosslinks. *Soft Matter* **2015**, *11*, 6152–6161.
- (21) Drahonovsky, D.; Lehn, J. M. Hemiacetals in Dynamic Covalent Chemistry: Formation, Exchange, Selection, and Modulation Processes. *J. Org. Chem.* **2009**, *74*, 8428–8432.
- (22) Kulchat, S.; Lehn, J. M. Dynamic Covalent Chemistry of Nucleophilic Substitution Component Exchange of Quaternary Ammonium Salts. *Chem. - Asian J.* **2015**, *10*, 2484–2496.
- (23) Bapat, A. P.; Roy, D.; Ray, J. G.; Savin, D. A.; Sumerlin, B. S. Dynamic-Covalent Macromolecular Stars with Boronic Ester Linkages. *J. Am. Chem. Soc.* **2011**, *133*, 19832–19838.
- (24) Montarnal, D.; Capelot, M.; Tournilhac, F.; Leibler, L. Silica-Like Malleable Materials from Permanent Organic Networks. *Science* **2011**, *334*, 965–968.
- (25) Lehn, J. M. Perspectives in Chemistry—Steps Towards Complex Matter. *Angew. Chem., Int. Ed.* **2013**, *52*, 2836–2850.
- (26) Roy, N.; Bruchmann, B.; Lehn, J. M. Dynamers: Dynamic Polymers as Self-Healing Materials. *Chem. Soc. Rev.* **2015**, *44*, 3786–3807.
- (27) Billiet, S.; De Bruycker, K.; Driessen, F.; Goossens, H.; Van Speybroeck, V.; Winne, J. M.; Du Prez, F. E. Triazolinediones Enable Ultrafast and Reversible Click Chemistry for the Design of Dynamic Polymer Systems. *Nat. Chem.* **2014**, *6*, 815–821.
- (28) de Hatten, X.; Bell, N.; Yufa, N.; Christmann, G.; Nitschke, J. R. A Dynamic Covalent, Luminescent Metallopolymer that Undergoes Sol-to-Gel Transition on Temperature Rise. *J. Am. Chem. Soc.* **2011**, *133*, 3158–3164.
- (29) Skene, W. G.; Lehn, J. M. Dynamers: Polyacylhydrazone Reversible Covalent Polymers, Component Exchange, and Constitutional Diversity. *Proc. Natl. Acad. Sci. U. S. A.* **2004**, *101*, 8270–8275.
- (30) Scott, T. F.; Schneider, A. D.; Cook, W. D.; Bowman, C. N. Photoinduced Plasticity in Cross-Linked Polymers. *Science* **2005**, *308*, 1615–1617.
- (31) Kloxin, C. J.; Scott, T. F.; Park, H. Y.; Bowman, C. N. Mechanophotopatterning on a Photoresponsive Elastomer. *Adv. Mater.* **2011**, *23*, 1977–1981.
- (32) Yang, C.; Wang, X.; Yao, X.; Zhang, Y.; Wu, W.; Jiang, X. Hyaluronic Acid Nanogels with Enzyme-sensitive Cross-linking Group for Drug Delivery. *J. Controlled Release* **2015**, *205*, 206–217.
- (33) Denissen, W.; Winne, J. M.; Du Prez, F. E. Vitrimers: Permanent Organic Networks with Glass-Like Fluidity. *Chem. Sci.* **2016**, *7*, 30–38.
- (34) Fortman, D. J.; Brutman, J. P.; Cramer, C. J.; Hillmyer, M. A.; Dichtel, W. R. Mechanically Activated, Catalyst-Free Polyhydroxyurethane Vitrimers. *J. Am. Chem. Soc.* **2015**, *137*, 14019–14022.
- (35) Denissen, W.; Rivero, G.; Nicolaÿ, R.; Leibler, L.; Winne, J. M.; Du Prez, F. E. Vinylogous Urethane Vitrimers. *Adv. Funct. Mater.* **2015**, *25*, 2451–2457.
- (36) Smallenburg, F.; Leibler, L.; Sciortino, F. Patchy Particle Model for Vitrimers. *Phys. Rev. Lett.* **2013**, *111*, 188002.
- (37) Garcia, J. M.; Jones, G. O.; Virwani, K.; McCloskey, B. D.; Boday, D. J.; ter Hurne, G. M.; Horn, H. W.; Coady, D. J.; Bintaleb, A. M.; Alabdulrahman, A. M. S.; Alsewaleh, F.; Almegren, H. A. A.; Hedrick, J. L. Recyclable, Strong Thermosets and Organogels via Paraformaldehyde Condensation with Diamines. *Science* **2014**, *344*, 732–735.
- (38) Dunetz, J. R.; Magano, J.; Weisenburger, G. A. Large-Scale Applications of Amide Coupling Reagents for the Synthesis of Pharmaceuticals. *Org. Process Res. Dev.* **2016**, *20*, 140–177.
- (39) Karan, S.; Jiang, Z.; Livingston, A. G. Membrane Filtration. Sub-10 nm Polyamide Nanofilms with Ultrafast Solvent Transport for Molecular Separation. *Science* **2015**, *348*, 1347–1351.
- (40) Pattabiraman, V. R.; Bode, J. W. Rethinking Amide Bond Synthesis. *Nature* **2011**, *480*, 471–479.
- (41) El-Faham, A.; Albericio, F. Peptide Coupling Reagents, More Than a Letter Soup. *Chem. Rev.* **2011**, *111*, 6557–6602.
- (42) Wang, H.-H.; Wu, S.-P. Synthesis of Thermally Stable Aromatic Poly(imide amide benzimidazole) Copolymers. *J. Appl. Polym. Sci.* **2003**, *90*, 1435–1444.
- (43) Balachandra, C.; Sharma, N. K. Instability of Amide Bond Comprising the 2-Aminotropone Moiety: Cleavable under Mild Acidic Conditions. *Org. Lett.* **2015**, *17*, 3948–3951.
- (44) Szostak, M.; Yao, L.; Aube, J. Stability of Medium-Bridged Twisted Amides in Aqueous Solutions. *J. Org. Chem.* **2009**, *74*, 1869–1875.
- (45) Hutchby, M.; Houlden, C. E.; Haddow, M. F.; Tyler, S. N. G.; Lloyd-Jones, G. C.; Booker-Milburn, K. I. Switching Pathways: Room-Temperature Neutral Solvolysis and Substitution of Amides. *Angew. Chem., Int. Ed.* **2012**, *51*, 548–551.
- (46) Aube, J. A New Twist on Amide Solvolysis. *Angew. Chem., Int. Ed.* **2012**, *51*, 3063–3065.

- (47) Zhang, D.; Zhou, J.; Xia, F.; Kang, Z.; Hu, W. Bond Cleavage, Fragment Modification and Reassembly in Enantioselective Three-Component Reactions. *Nat. Commun.* **2015**, *6*, 5801.
- (48) Serafimova, I. M.; Pufall, M. A.; Krishnan, S.; Duda, K.; Cohen, M. S.; Maglathlin, R. L.; McFarland, J. M.; Miller, R. M.; Frödin, M.; Taunton, J. Reversible Targeting of Noncatalytic Cysteines with Chemically Tuned Electrophiles. *Nat. Chem. Biol.* **2012**, *8*, 471–476.
- (49) Krishnan, S.; Miller, R. M.; Tian, B.; Mullins, R. D.; Jacobson, M. P.; Taunton, J. Design of Reversible, Cysteine-Targeted Michael Acceptors Guided by Kinetic and Computational Analysis. *J. Am. Chem. Soc.* **2014**, *136*, 12624–12630.
- (50) ASTM Standard D-4065-01, “Standard Practice for Plastics: Dynamic Mechanical Properties: Determination and Report of Procedure”, ASTM International, 2000.
- (51) Rousseau, O.; Delaunay, T.; Robiette, R. Synthesis of Monosubstituted 1,1-Dicarbonyl Ester 1,3-Dienes. *Synlett* **2014**, *25*, 519–522.
- (52) Kuhnert, M.; Köster, H.; Bartholomäus, R.; Park, A. Y.; Shahim, A.; Heine, A.; Steuber, H.; Klebe, G.; Diederich, W. E. Tracing Binding Modes in Hit-to-Lead Optimization: Chameleon-Like Poses of Aspartic Protease Inhibitors. *Angew. Chem., Int. Ed.* **2015**, *54*, 2849–2853.
- (53) Wurthner, F.; Yao, S.; Debaerdemaeker, T.; Wortmann, R. Dimerization of Merocyanine Dyes. Structural and Energetic Characterization of Dipolar Dye Aggregates and Implications for Nonlinear Optical Materials. *J. Am. Chem. Soc.* **2002**, *124*, 9431–9447.
- (54) Ying, A.; Li, Z.; Yang, J.; Liu, S.; Xu, S.; Yan, H.; Wu, C. DABCO-Based Ionic Liquids: Recyclable Catalysts for Aza-Michael Addition of α,β -Unsaturated Amides Under Solvent-Free Conditions. *J. Org. Chem.* **2014**, *79*, 6510–6516.
- (55) Both TPMD and Oligoamines Formed a Homogeneous Mixture at Room Temperature for any Mole% of TMPD between 30–50 in the Mixture.
- (56) www.engineeringtoolbox.com/young-modulus-d_417.html.
- (57) Kamata, H.; Akagi, Y.; Kayasuga-Kariya, Y.; Chung, U. I.; Sakai, T. “Nonswellable” Hydrogel without Mechanical Hysteresis. *Science* **2014**, *343*, 873–875.
- (58) The time constants (τ) of the exponential decay were evaluated by fitting the terminal part of the curves to the function $\exp(-t/\tau)$.
- (59) Adams, J. M.; Mao, Y.; Vandoolaeghe, W. L. Stress Relaxation in Polymer Networks: Equilibrium Behavior and Dynamics. *J. Chem. Phys.* **2007**, *127*, 114907.
- (60) Papadopoulou, E. L.; Pignatelli, F.; Marras, S.; Marini, L.; Davis, A.; Athanassiou, A.; Bayer, I. S. Nylon 6,6/graphene nanoplatelet composite films obtained from a new solvent. *RSC Adv.* **2016**, *6*, 6823–6831.
- (61) Kuo, M.-C.; Tung, Y.-C.; Yeh, C.-L.; Chang, H.-Y.; Jeng, R.-J.; Dai, S. A. Synthesis and Rapid Polymerizations of Aryl- and Alkyl-bis(azetidine-2,4-dione)s to Polymalonamide Elastomers. *Macromolecules* **2008**, *41*, 9637–9642.
- (62) Levchik, G. F.; Si, K.; Levchik, S. V.; Camino, G.; Wilkie, C. A. The Correlation Between Cross-linking and Thermal Stability: Cross-linked Polystyrenes and Polymethacrylates. *Polym. Degrad. Stab.* **1999**, *65*, 395–403.
- (63) Allen, C. L.; Chhatwal, A. R.; Williams, J. M. J. Direct Amide Formation from Unactivated Carboxylic Acids and Amines. *Chem. Commun.* **2012**, *48*, 666–668.
- (64) Rahman, M.; Kundu, D.; Hajra, A.; Majee, A. Formylation without Catalyst and Solvent at 80 °C. *Tetrahedron Lett.* **2010**, *51*, 2896–2899.